arXiv:cond-mat/0511120v1 [cond-mat.str-el] 4 Nov 2005

Antiferromagnetic fluctuations, symmetry and shape of the gap function in the electron-doped superconductors: the functional renormalization-group analysis

A. A. Katanin[a,b]
[a] *Max-Planck-Institut für Festkörperforschung, D-70569 Stuttgart, Germany*
[b] *Institute of Metal Physics, 620219 Ekaterinburg, Russia*

The problem of the symmetry of the superconducting pairing and the form of the gap function in the electron-doped superconductors is reconsidered within the temperature-cutoff functional renormalization group approach combined with the Bethe-Salpeter equations. The momentum dependence of the order parameter for antiferromagnetic and superconducting instabilities in these compounds is analyzed. The gap function in the antiferromagnetic (particle-hole) channel has its maxima at the hot-spots, or at the diagonal of the Brilloin zone in their absence. The wavefunction in the singlet superconducting channel is non-monotonic in the vicinity of the $(\pi,0)$ and $(0,\pi)$ points, deviating therefore from the conventional d-wave form in striking similarity with recent experimental data. An instability in the triplet superconducting channel is much weaker than the singlet one and has an f-wave like form of the gap function.

PACS Numbers: 71.10.Fd; 71.27.+a;74.25.Dw

It is by now well established that the superconducting order parameter in high-T$_c$ compounds is described by a nearly $(\cos k_x - \cos k_y)$-momentum dependence: its absolute value is largest at the Fermi surface (FS) points close to $(\pi,0)$ and $(0,\pi)$ and vanishes at the FS crossings on the Brillouin zone (BZ) diagonals.

Accurate measurements of the gap function in the hole-doped cuprates found, however, a slight deviation from this d$_{x^2-y^2}$-wave momentum dependence [1], with a flatter angular dependence near the nodal points. On the other hand, recent experiments on the electron-doped cuprates revealed non-monotonicity of the gap function as a function of an angle around the FS [2,3]. In particular, the observed gap function has its maxima away from the points of the Fermi surface which are closest to the $(\pi,0)$ and $(0,\pi)$ points of the Brillouin zone. Since the symmetry and the details of the momentum dependence of the superconducting order parameter are closely related to the structure of the effective pairing interaction between the electrons, the momentum dependence of the gap function contains important information about the pairing mechanism in high-T_c compounds.

One of the proposed candidates for the pairing mechanism in cuprates is the antiferromagnetic (AFM) spin fluctuations scenario [4–7]. While the theoretical studies of the hole-doped compounds found that antiferromagnetic fluctuations lead to a d-wave symmetry of the gap function [8,9], there is currently a theoretical controversy about the symmetry of the superconducting pairing in the electron-doped cuprates. As it was argued earlier [2,3], with increasing electron doping the hot-spots of the Fermi surface (i.e. the points connected by the antiferromagnetic wave vector $\mathbf{Q}=(\pi,\pi)$) move towards each other (see Fig.1a). Since the sign of the d-wave gap is opposite at the hot-spots, this leads to the suppression of the tendency towards the d-wave pairing.

In this situation, different types of the pairing symmetry were proposed. An s-wave pairing at large electron dopings was proposed [10], as arising mainly due to the effect of disorder in the model with both short- and long-range Coulomb parts of the interaction. On the other hand, for short-range interactions in the absence of disorder, p-wave superconductivity was considered as a possible candidate in the presence of strong charge fluctuations [11]. With these theoretical proposals, it remains an important problem which pairing symmetry is favored at intermediate and large electron dopings and what is the theoretically expected ground state superconducting order parameter for the electron-doped superconductors.

To study this problem, we apply in the present paper the functional renormalization-group (fRG) technique [12–16], which proved successful in describing the interplay of antiferromagnetism and d-wave superconductivity in the *t*-*t*′ Hubbard model. Although a previous application of this technique to the microscopic analysis of electron-doped superconductors within the Hubbard model found d-wave pairing even at relatively high dopings [17], the results of this study will be reconsidered in the present paper in two points.

First, the momentum-cutoff renormalization group approach of Ref. [17] does not allow to search for the charge and spin instabilities in the forward scattering (zero-momentum transfer) channel. This approach, therefore, may miss the possibility of the triplet pairing, which is often closely related to such instabilities. This drawback is overcome in the temperature-cutoff fRG approach [15], which uses temperature as a natural cutoff parameter and proved successful in describing both AFM and ferromagnetic instabilities together with singlet- and triplet superconducting pairing [15,16].

Second, a recent extension of the temperature cutoff renormalization group approach - its combination with

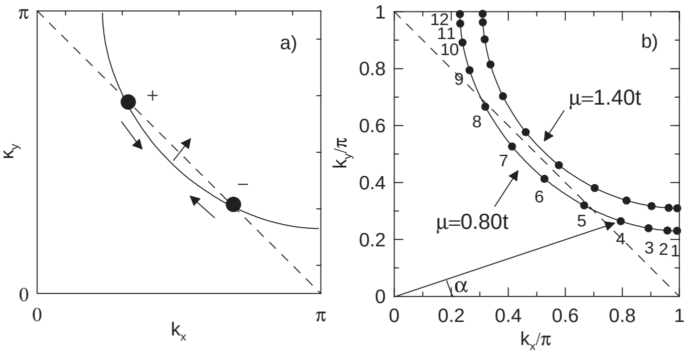

FIG. 1. (a) The shape of the Fermi-surface (solid line) in the electron-doped superconductors, the dashed line shows the umklapp surface $k_x + k_y = \pi$, black circles mark hot-spots, arrows indicate the direction of movement of the Fermi-surface and hot-spots with increasing doping. (b) The actual non-interacting Fermi surfaces of the model (1) at $t' = 0.3t$, and $\mu = 0.8t$ ($\delta = n - 1 = 0.09$) and $\mu = 1.4t$ ($\delta = 0.26$). The dots mark the positions of the centers of 12 patches, located in the upper-right quarter of the Brilloin zone; α is an angle corrdinate of the patch centers.

the Bethe-Salpeter (BS) approach - was proposed as a very convenient tool of studing symmetry and the form of the wavefunctions of different order parameters [18]. Contrary to previous fRG approaches, this method is not based on the knowledge of the wavefunctions at high temperatures. For the hole-doped superconductors it predicts correctly the flattening of the gap function near the nodal points [18] in agreement with the experimental observation [1].

In the present paper we use the temperature cutoff functional renormalization group approach in combination with the Bethe-Salpeter equations to extract eigenfunctions and eigenvalues of the effective interaction in the particle-particle (pp) or the particle-hole (ph) channel in the electron-doped superconductors.

The model. As a convenient model which describes electron-doped superconductors, we consider the 2D t-t' Hubbard model $H_\mu = H - (\mu - 4t')N$ with

$$H = -\sum_{ij\sigma} t_{ij} c^\dagger_{i\sigma} c_{j\sigma} + U \sum_i n_{i\uparrow} n_{i\downarrow} \qquad (1)$$

where $t_{ij} = t$ for nearest neighbor (nn) sites i and j and $t_{ij} = -t'$ for next-nn sites ($t, t' > 0$) on a square lattice. The chemical potential μ is determined by the filling $n > 1$; for convenience we have shifted the chemical potential μ by $4t'$.

The method. We follow the many-patch temperature cutoff fRG for one-particle irreducible Green functions as proposed in Ref. [15]. This scheme accounts for excitations with momenta far from and close to the FS, which is necessary for the description of instabilities arising from zero-momentum transfer ph scattering. The momentum dependence of the effective interaction between electrons at a given temperature, $V_T(\mathbf{k}_1, \mathbf{k}_2, \mathbf{k}_3, \mathbf{k}_4)$ is parametrized by the position of incoming $\mathbf{k}_1, \mathbf{k}_2$ and outgoing electron momentum $\mathbf{k}_3$ at the Fermi surface. The fourth momentum, $\mathbf{k}_4$ is determined by the momentum conservation law. Neglecting the frequency dependence of the vertices, which is expected to have minor relevance in the weak-coupling regime, the RG differential equation for the interaction vertex has the form [15]

$$\frac{\mathrm{d}V_T}{\mathrm{d}T} = -V_T \circ \frac{\mathrm{d}L_{\mathrm{pp}}}{\mathrm{d}T} \circ V_T + V_T \circ \frac{\mathrm{d}L_{\mathrm{ph}}}{\mathrm{d}T} \circ V_T \,, \qquad (2)$$

where $\circ$ is a short notation for summations over intermediate momenta and spin,

$$L_{\mathrm{ph,pp}}(\mathbf{k}, \mathbf{k}') = \frac{f_T(\varepsilon_\mathbf{k}) - f_T(\pm\varepsilon_{\mathbf{k}'})}{\varepsilon_\mathbf{k} \mp \varepsilon_{\mathbf{k}'}}, \qquad (3)$$

and $f_T(\varepsilon)$ is the Fermi function. The upper sign in Eq.(3) is for L_{ph} and the lower sign for L_{pp}, respectively. Eq.(2) has to be solved with the initial condition $V_{T_0}(\mathbf{k}_1, \mathbf{k}_2, \mathbf{k}_3, \mathbf{k}_4) = U$; the initial temperature is chosen as large as $T_0 = 400t$.

We discretize the momentum space in $N_p = 48$ patches using the same patching scheme as in Ref. [15]. This reduces the integro-differential equations (2) to a set of 5824 differential equations, which were solved numerically. The position of the centers of the patches at the Fermi surface for two different filling is shown in Fig. 1b.

To perform an analysis of possible instabilities within the fRG+BS approach, we consider the solution of the Bethe-Salpeter equations [18,19]

$$\begin{aligned} \sum_\mathbf{p} \Gamma^T_{\mathrm{ph}}(\mathbf{k}, \mathbf{p}) L_{\mathrm{ph}}(\mathbf{p}, \mathbf{p} + \mathbf{Q}) \phi^{\mathrm{ph}}_\mathbf{p} &= \frac{\lambda_{\mathrm{ph}} \phi^{\mathrm{ph}}_\mathbf{k}}{1 - \lambda_{\mathrm{ph}}} \,, \\ -\sum_\mathbf{p} \Gamma^T_{\mathrm{pp}}(\mathbf{k}, \mathbf{p}) L_{\mathrm{pp}}(\mathbf{p}, -\mathbf{p}) \phi^{\mathrm{pp}}_\mathbf{p} &= \frac{\lambda_{\mathrm{pp}} \phi^{\mathrm{pp}}_\mathbf{k}}{1 - \lambda_{\mathrm{pp}}} \,, \end{aligned} \qquad (4)$$

The 2-particle reducible vertices $\Gamma^T_{\mathrm{ph,pp}}(\mathbf{k}, \mathbf{k}')$ can be directly extracted from the fRG flow according to

$$\Gamma^T_{\mathrm{ph,pp}}(\mathbf{k}, \mathbf{k}') = \left\{ \begin{array}{l} V_T(\mathbf{k}, \mathbf{k}', \mathbf{k}' + \mathbf{Q}), \quad \text{ph (AFM)} \\ V_T(\mathbf{k}, -\mathbf{k}, \mathbf{k}') \pm V_T(\mathbf{k}, -\mathbf{k}, -\mathbf{k}'), \\ \qquad\qquad \text{pp (singlet, triplet SC)} \end{array} \right. \qquad (5)$$

The value $\lambda_{\mathrm{ph,pp}} = 1$ corresponds to an ordering instability with the symmetry of the eigenfunction $\phi^{\mathrm{ph,pp}}_\mathbf{k}$. Therefore, tracing the temperature dependence of eigenvalues and -functions allows to identify both, the leading instabilities *and* their concomitant order parameter structure. We stop the fRG flow at the temperature $T_X = 0.001t$ (the maximum interaction vertex $V_{\max} \equiv \max\{V(\mathbf{k}_1, \mathbf{k}_2; \mathbf{k}_3, \mathbf{k}_4)\}$ at this temperature remains smaller than the bandwidth). We have verified that the results for the eigenfunctions are only weakly dependent on the choice of T_X.

Results. Below we discuss the results of the numerical solution of the Bethe-Salpeter equations in the electron-doping regime. We choose $t' = 0.3t$ which is close to typical values considered for the electron- doped cuprates.

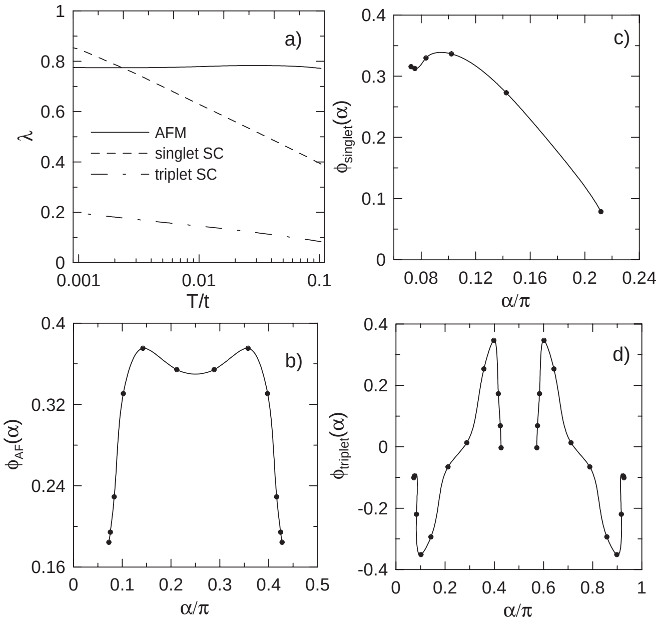

FIG. 2. Eigenvalues (a) and angular-dependence on the FS of the eigenfunctions $\phi_{\mathbf{p}}$ of the Bethe-Salpeter equation at $T = T_X$ (b,c,d) for $t' = 0.3t$, $U = 3.5t$, $\mu = 0.8t$ ($\delta = 0.09$). T_X is the lowest temperature reached in the fRG flow. The dots are the value of the eigenfunctions at the centers of corresponding patches, cf. Fig. 1

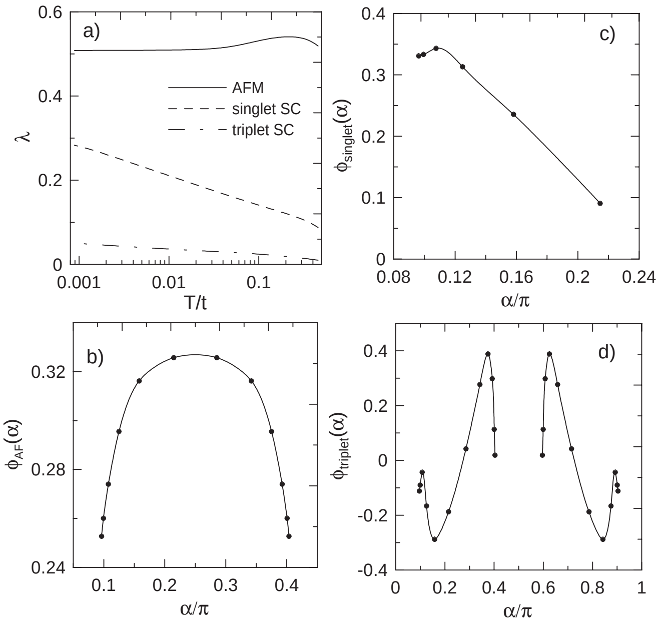

FIG. 3. Same as Fig. 2 for $\mu = 1.4t$ ($\delta = 0.26$).

To remain in the weak-coupling regime, where the considered technique is applicable, we put $U = 3.5t$. Although this value is substantially smaller than that which is expected for the cuprate materials, we show that it allows us to reproduce the main features which are observed experimentally. We also do not expect qualitative change of the results even for higher values of U.

We start in Fig. 2 with the results for the chemical potential $\mu = 0.8t$, which corresponds to a filling $n = 1.09$, i.e. 9% of the electron doping. At this filling the eigenvalue corresponding to the AFM instability saturates at a value $\lambda < 1$ at the smallest temperature T_X which one can reach in the fRG flow. Therefore, the AFM is not expected to be the leading ground-state instability (more generally, the AFM is found not to dominate at $\mu > 0.7t$, i.e. $\delta > 0.05$). The corresponding eigenfunction in the particle-hole channel (Fig. 2b) has its maxima at the hot-spots of the Fermi surface.

The eigenvalue λ_{pp} in the singlet pairing channel is monotonically increasing with decreasing temperature, and it is biggest close to T_X. Therefore, the singlet pairing is expected to be the leading instability at $T \to 0$. The corresponding wave function is non-monotonic (Fig. 2c) and has a shape which is strikingly similar to the recent experimental data [2,3]. The maximum of the wavefunction lies between the 3-rd and 4-th patch of the Fermi surface, i.e. it is shifted from the position of the hot-spot towards the point of the FS closest to the $(\pi, 0)$. The eigenvalue corresponding to the triplet pairing instability is much smaller than for the singlet one, although it increases with decreasing temperature. The corresponding wave function (Fig. 2d) has nodes at the diagonals, and it is maximal near hot spots having therefore f-wave like symmetry.

Now we consider the case of stronger doping $\mu = 1.40t$, i.e. $n = 1.26$ (26% of the electron doping), see Fig. 3. In this case the hot-spots of the Fermi surface are absent. The eigenvalue corresponding to the AFM instability is decreasing with decreasing temperature at low T, so that this instability is again not favored in the ground state. The corresponding eigenfunction has its maximum at the diagonal of the Brillouin zone. Both eigenvalues corresponding to the singlet- and triplet superconducting pairing are smaller than in the case of $\mu = 0.80t$, although the singlet superconductivity remains the leading instability in the $T \to 0$ limit. The shapes of the wavefunctions for singlet and triplet pairing are similar to those at $\mu = 0.80t$. The maximum of the wavefunction in the singlet superconducting channel is further shifted towards the $(\pi, 0)$ point of the Brillouin zone (i.e. in the direction opposite to the hot-spots), while maxima of the eigenfunction in the triplet pairing channel are shifted towards the diagonal.

Now we discuss the physical origin of the shape of the gap functions found in the numerical analysis. To this end, we plot the effective pairing interaction $\Gamma^{T}_{pp}(\mathbf{k}, \mathbf{k}')$ in the singlet- and triplet channel as a function of the momenta $\mathbf{k}, \mathbf{k}'$ on the Fermi surface (Fig.4). One can see that at low electron doping ($\mu = 0.8t$) the maxima of the attractive interaction in both, the singlet and the triplet channels are located near the hot-spots (Fig. 4a,b), which leads to the maximum of the pairing gap near these points. The difference in 1 patch between the

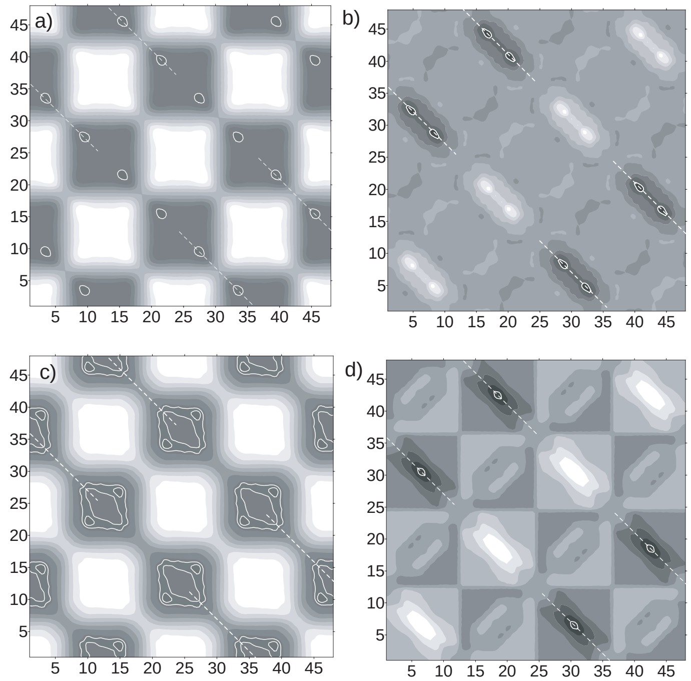

FIG. 4. Contour plots of the pairing interaction $\Gamma^{T}_{pp}(\mathbf{k},\mathbf{k}')$ in singlet (a,c) and triplet (b,d) channels at $t' = 0.3t$, $U = 3.5t$, $\mu = 0.8t$ (a,b) and $\mu = 1.4t$ (c,d) as a function of the position of the momenta $\mathbf{k},\mathbf{k}'$ at the Fermi surface (labeled by the number of patch). Black color corresponds to the attractive (negative), white - to the repulsive (positive) interaction. White contours show regions with the strongest attraction, dashed lines mark the points with $\mathbf{k}_{x,y} = -\mathbf{k}'_{y,x}$.

position of the hot-spots and the maxima of the gaps can be explained in this case by small incommensurability of spin fluctuations and the contribution of the other channels of electronic scattering. With increasing doping the maximum of the interaction in the singlet channel spreads in a broader momentum range (Fig. 4c), which, however, leads to almost the same position of the maxima of the gap, as for small electron doping. The maximum of the attraction in the triplet channel at the points with $\mathbf{k}_{x,y} = -\mathbf{k}'_{y,x}$ shifts towards the diagonal of the Brillouin zone, where it is compensated, however, by the strong repulsion, which arises at $\mathbf{k} = \mathbf{k}'$ (Fig. 4d). As a "compromise", the maxima of the gap are located in the parts of the momentum space where neither repulsive nor attractive interaction is strong, i.e. again remain almost unchanged with respect to small doping.

Therefore, while at small doping the shape of the gap functions are determined by the spin fluctuations with the wavevector close to $\mathbf{Q}$, at larger dopings the spin fluctuations with broader range of momenta start to play an important role. Note that the maximum of the singlet gap is located away from the Fermi surface points closest to $(\pi, 0)$ and $(0, \pi)$ only for the fillings $n > 1$; on the hole doped side (i.e. at fillings $n < 1$) the nonmonotonicity of the singlet gap function quickly disappears [18].

In conclusion, we have investigated the symmetry of the leading instabilities and the shape of the corresponding wavefunctions of the 2D electron doped superconductors within the 2D t-t' Hubbard model using as a novel tool the combination of the Bethe-Salpeter equation and the fRG approach. At $U = 3.5t$ we have found the d-wave pairing instability to be the strongest instability for dopings $\delta > 0.05$ (one can expect that the range of dopings where the AFM instability is the leading one, increases further with increasing interaction strength). The angular dependence of the singlet pairing gap function is found to be non-monotonic and its shape is strikingly similar to the recent experimental data. The position of the maximum of the gap is close to the position of the hot spots at low doping level and deviates from it at higher dopings, where the antiferromagnetic fluctuations with wavevectors with broad momenta range become essential. The triplet instability has subleading eigenvalues and f-wave like form of the wavefunction. The maxima of the wavefunction are close to the hot-spots at low electron dopings and are close to the diagonal for higher dopings.

I am grateful to V. M. Yakovenko for stimulating discussions and pointing my attention to the problem of electron-doped cuprates and to the ICCMP (Brasilia) where this work was initiated.

---

[1] J. Mesot et al., Phys. Rev. Lett. **83**, 840 (1999).
[2] G. Bluemberg et al., Phys. Rev. Lett. **88**, 107002 (2002).
[3] H. Matsui et al., Phys. Rev. Lett. **95**, 017003 (2005).
[4] D. J. Scalapino, J. Low Temp. Phys. **117,** 179 (1999).
[5] N. E. Bickers, et al., Phys. Rev. Lett. **62,** 961 (1989).
[6] J. Schmalian, et al., Phys. Rev. Lett. **80,** 3839 (1998).
[7] A. Chubukov and D. Morr, Phys. Rep. **288**, 355 (1997); A. Abanov et al., Phys. Rev. Lett. **84**, 5608 (2000).
[8] D. J. Scalapino, et al., Phys. Rev. B **34**, 8190 (1986); ibid. **35**, 6694 (1987).
[9] S. R. White et al., Phys. Rev. B **39**, 839 (1989); N. Bulut et al., Phys. Rev. B **47**, 2742 (1993)
[10] A. A. Abrikosov, Phys. Rev. B **53**, R8910 (1996); ibid. **52**, R15738 (1995)
[11] V. A. Khodel, et. al., Phys. Rev. B **69**, 144501 (2004).
[12] D. Zanchi and H.J. Schulz, Phys. Rev. B **54**, 9509 (1996); ibid. **61**, 13609 (2000).
[13] C. J. Halboth and W. Metzner, Phys. Rev. B **61**, 7364 (2000); Phys. Rev. Lett. **85**, 5162 (2000).
[14] C. Honerkamp, et al., Phys. Rev. B **63**, 035109 (2001).
[15] C. Honerkamp and M. Salmhofer, Phys. Rev. Lett. **87**, 187004 (2001); Phys. Rev. B **64**, 184516 (2001).
[16] A. A. Katanin and A. P. Kampf, Phys. Rev. B **68**, 195101 (2003); ibid. **67**, 125104 (2003).
[17] C. Honerkamp, Eur. Phys. J. B **21**, 81 (2001).
[18] A. A. Katanin and A. P. Kampf, cond-mat/0408246 (unpublished); Phys. Rev. B. in press.
[19] N. Bulut, D. J. Scalapino, and S. R. White, Phys. Rev. B **47**, 6157 (1993); ibid. **47**, 14599 (1993).